Comparative Study of Integer- and Fractional-Order PID Controller Tuning for BLDC Motor Speed Using Single- and Multi-Objective Optimization

Assia Boubidi and Sihem Kechida

Laboratoire d'Automatique et Informatique de Guelma (LAIG), Université 8 Mai 1945, BP 401 Guelma 24000, Algeria.

Abstract— This paper presents an optimal design of Integer- and Fractional-Order Proportional-Integral-Derivative (PID/FOPID) controller parameters for speed control of BLDC motor based on Single- and Multi-Objective Optimization (SOO/MOO). For SOO, the process of tuning was conducted via the Whale Optimization Algorithm (WOA) under Integral of Time Absolute Error (ITAE) objective function. At the end of SOO, the best solution which corresponds to PID/FOPID controller's gains values has been obtained directly according to the minimum value of ITAE objective function. For MOO, the Multi-Objective Whale Optimization Algorithm (MOWOA) was used with three objective functions to minimize which are: settling time, overshoot and error steady state. The MOO generates non-dominated solutions forming Pareto front. The best compromise solution was obtained using fuzzy decision-making approach satisfying desired preferences. For the comparison of different controllers, step responses, frequency responses, tracking and load disturbance responses were all carried out and analyzed. The simulation results have shown that the MOWOA-FOPID controller provides a better response with faster speed without any overshoots, and good tracking capacity rejecting the load disturbances.

Keywords— BLDC motor speed control, single- and multi-objective optimization, fractional-order PID, whale optimization algorithm. Multi-Objective whale optimization algorithm.

I Introduction

The BLDC motors are typically permanent magnet synchronous motor, they are well driven by DC voltage and they are electronically commutated motors. Some of the advantages of BLDC motors are their higher speed ranges, higher efficiency, better speed versus torque characteristics, long operating life, noiseless operation, etc [1].

In high performance drive applications, such as in the areas of robotic, machine tools and rolling mills, BLDC motor is desired to operate at various speed and load conditions with enhanced performances and robust speed control [2]. In the last decades, a lot of controllers have been suggested for BLDC motor speed control such as PI [3-6], PD [7], PID [8-12], Fuzzy Logic [13-16], LQR [17], etc. However, the most popular technique is the PID controller because of its simple structure, strong robustness, and good applicability [18]. The basic PID configuration is made up of three terms: proportional gain (K_p), integration gain (K_i) and derivative gains (K_d). These three parameters can be adjusted to realize the desired objective of the control process [19].

For few decades, the field of control theory has been dominated with integer-order controllers. With the development of fractional calculus, fractional-order integral and differential have introduced in control applications to offer more flexibility to control design. Therefore, control theory has paved way to migrate from classical controllers which are integer-order to fractional-order controllers. In 1999, Podlubny [20] has proposed a generalization of PID controllers, namely the fractional-order PID (FOPID) controller. The FOPID controller noted $\mathrm{PI}^{\lambda}\mathrm{D}^{\mu}$ is a conventional PID controller whose integration action order λ and differentiation action order μ are real rather than integer. Therefore, FOPID controller beside the proportional, integral and derivative parameters (K_p, K_i and K_d) it has two additional parameters which are λ and μ. This expansion adds more robustness and flexibility to control system [21-23]. Compared with conventional PID controller, FOPID controller offers much more versatility in tuning and therefore, has a large area of parameters that govern the controlled system and increases the reliability of the control loop [24,25].

In recent years, metaheuristic optimization techniques have been widely used in the controller tuning in both single- and multi-objective optimization framework such as genetic algorithms (GA), particle swarm optimization (PSO), ant colony optimization (ACO), whale optimization algorithm (WOA), differential evolution (DE), and the cuckoo search (CS) algorithms, etc. In the single-objective optimization, one function is used to be optimized such as standard performance indices; integral of absolute error (IAE), integral of time absolute error (ITAE), integral of squared error (ISE), integral of time squared error (ITSE), and integral of squared time squared error (ISTE) [26]. Each one of them has advantages and disadvantages. For example, since IAE and ISE criteria are independent of time, the obtained results have relatively small overshoot but a long settling time. The ITAE and ITSE performance criteria can overcome this drawback, but they cannot ensure to have a desirable stability margin [26]. To address this shortcoming, multi-objective optimization has lately introduced to control theory. It optimizes different functions simultaneously to obtain the best solution. Objective functions are based on the performance indices of the system output. These functions usually involve the time domain performance criterion; the maximum overshoot (Mp), rise time (tr), settling time (ts), and steady-state error (ess). There are two kinds of methods commonly used: the scalarization method and the Pareto method. The scalarization method uses the weighting sum for separate objective functions. In this case, the multi-objective issue turned to one objective problem. However, the choice of the weighting factors in the objective function is not an easy task [27]. The Pareto method is the most popular multi-objective optimization method. It utilizes a trade-off among the objective functions based on the Pareto dominance concept. In Pareto dominance, the obtained solutions are classified into dominated and non-dominated solutions. Then the best solution can be chosen from the non-dominated solutions namely Pareto front by the decision-maker [28].

From literature review, for BLDC motor speed control there are some research articles [2,29,30] related to tuning of the FOPID parameters using single-objective function, but there is no work that has tried to optimize FOPID using multi-objective optimization approach. This motivated us to work in this area and benefit from the advantages of fractional-order controllers and multi-objective optimization to boost the performance of the control system.

In this paper, the optimal design of PID/FOPID controller parameters for speed control of BLDC motor is presented. The controller parameters are tuned through single- and multi-objective optimization algorithms which are WOA and MOWOA, respectively. For SOO, Integral of Time Absolute Error (ITAE) was taken as the main objective function to minimize. The best solution which corresponds to PID/FOPID controller's gains values has been obtained directly according to the minimum value of ITAE. While for MOO, three objective functions to minimize are employed which are: settling time, overshoot and error steady state. The best solution is determined by fuzzy logic-decision approach from the Pareto front archived by MOO. The main advantage of using fuzzy logic in the decision making is to give the decision maker more flexibility in determining the compromise solution changing the fuzzy rules regarding his preferences [31]. In order to compare the effectiveness of different controllers, speed step responses, frequency responses, tracking and load disturbance responses were all carried out and analyzed. The simulation results have shown that the MOWOA-FOPID controller provides a better response with faster speed without any overshoots, and good tracking capacity rejecting the load disturbances.

The paper is organized as follows: Section II presents the BLDC motor speed control system. Sections III and IV describe the PID/FOPID controller tuning using single-objective optimization with WOA algorithm and multi-objective optimization with MOWOA algorithm, respectively. Section V gives the simulation results. Finally, the conclusions are presented in Section VI.

II BLDC motor speed control system

A) Presentation

The conventional feedback control loop with parallel FOPID controller in bloc diagram form is shown in Fig 1. $G(s)$ is the plant-model of BLDC motor which will be presented in the next section. The output system $V(s)$ is the speed motor. $R(s)$ is the reference input and $D(s)$ is the charge disturbance. The controller receives the error signal $E(s)$ and generates control signal $U(s)$. It is represented by the transfer function as follows

$$C(s)|_{FOPID} = K_p + \frac{K_i}{s^\lambda} + K_d s^\mu, \qquad \lambda, \mu > 0 \tag{1}$$

$$C(s)|_{PID} = K_p + \frac{K_i}{s} + K_d s \tag{2}$$

where K_p is proportional gain, K_i is integration gain, K_d is derivative gain, λ is integration order and μ is derivative order. The conventional PID (2) can be obtained from FOPID controller with setting integration order λ and derivative order μ in equation (1) as 1 ($\lambda = 1$ and $\mu = 1$).

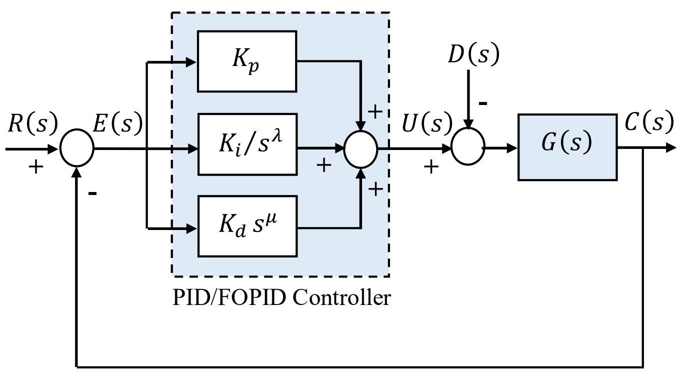

Fig. 1. The block diagram of BLDC motor speed control system.

B) BLDC motor model

Recently, Khluabwannarat et al. [32] were study a BLDC motor of 350 W, 24 VDC, 0.7 A, 300 rpm in their laboratory. Using the flower pollination algorithm (FPA) under the SSE objective function, the IO and FO models of such the BLDC motor were identified as stated in equations (3) and (4) respectively.

$$G(s)|_{IO} = \frac{148.80}{1.328s^3 + 13.05s^2 + 77.81s + 149.4} \tag{3}$$

$$G(s)|_{FO} = \frac{1.0}{0.029043s^{2.6582}+0.47836s^{1.2376}+1.1075s^{0.0443}} \tag{4}$$

Fig. 2 gives the step responses of the two models. A good agreement of IO-model to FO-model on the interval [0,5] is shown. Once evaluating their cost function values, the authors [32] were found that the FO-model is more accurate than the IO-model. Consequently, in their next work [29], FO-model was adopted to design the integer-order and fractional-order PID controller by using the same optimization algorithm (FPA) under the same objective function (SSE).

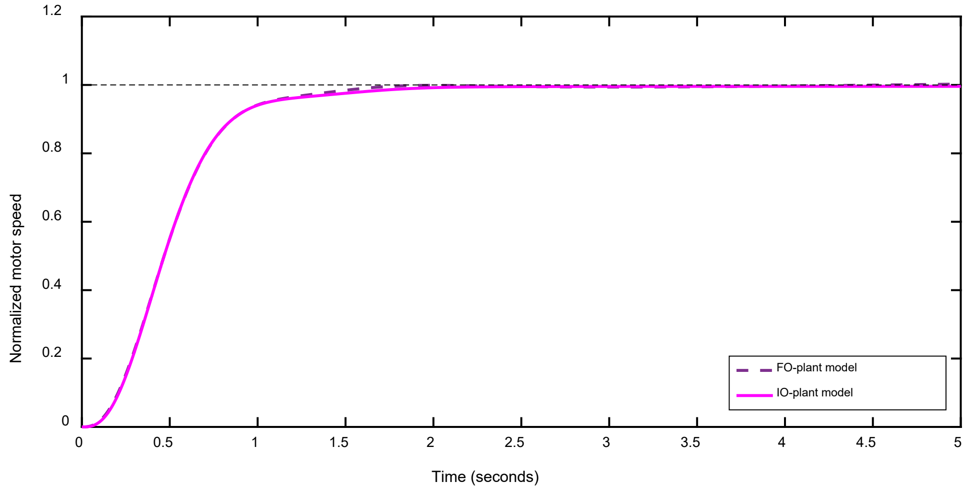

Fig. 2. Step responses of IO and FO-models on the interval [0,5].

Let's retake the transfer function of the FO-model (4). This function can be rewritten as

$$G(s)|_{FO} = \frac{1.0}{s^{0.044262}(0.029043s^{\,2.6139}+0.47836s^{1.1933} + 1.1075)} \tag{5}$$

At steady state, the FO-model becomes a pure integrator with 0.044262 order as follows

$$G(s)|_{FO,\ stady\ state} = \frac{1}{1.1075s^{0.044262}} \tag{6}$$

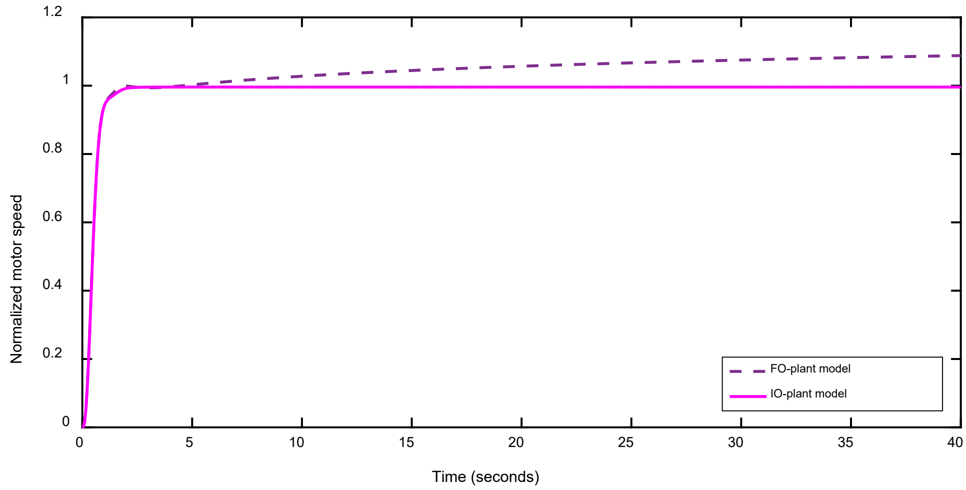

Fig. 3. Step responses of IO and FO-models on the interval [0,40].

Fig. 3 shows the step response plots of IO and FO-models, but this time over a larger range [0,40]. It is clear that the response of the FO-model increases indefinitely which does not represent the reality where the motor speed stabilizes at a finite value. Therefore, the FO-model that the authors [29,32] have chosen is not suitable to represent the motor.
In this paper, the BLDC motor is represented by IO-model (3) to design PID/FOPID controllers with single- and multi-objective optimization.

III PID/FOPID controller tuning using single-objective optimization

In this section, the optimal tuning of the PID/FOPID controller's parameters using single-objective optimization is presented. In control theory using single-objective optimization, one function is used to be optimized such as standard performance indices; integral of absolute error (IAE), integral of time absolute error (ITAE), integral of squared error (ISE), integral of time squared error (ITSE), and integral of squared time squared error (ISTE) [26]. The best solution which corresponds in this paper to PID/FOPID controller's gains values are obtained directly according to the minimum value of the adopted objective function. Fig. 4 shows different steps to design PID/FOPID controller parameters using SOO. In this paper, SOO is conducted via a metaheuristic optimization algorithm called the Whale Optimization Algorithm (WOA) under Integral of Time Absolute Error (ITAE) objective function.
Thereafter, objective function, single-objective optimization and a short explanation of WOA are given.

A) Objective function

In this paper, ITAE is used as objective function. It is defined as follow

$$ITAE = \int_0^{t_{sim}} t|e(t)|dt \tag{7}$$

with t_{sim} is the simulation time and $e(t)$ is the error signal as shown in Fig. 1.

B) Single-objective optimization steps

The SOO formulation is conducted using the following steps illustrated in Fig. 4.

Step 1: Initialize the population.
Step 2: Calculate the objective function for each individual in the population.
Step 3: Update the leader according to the minimum value of objective function.
Step 4: Increment iteration number.
If the criterion $(k \leq k_{max})$ has been satisfied, then:
- ✓ Update the population position by specified algorithm (WOA).
- ✓ Go to **Step 2**.

Otherwise, return the best solution which represents the leader.
endif

C) Whale Optimization Algorithm

Whale optimization algorithm (WOA) is a recently meta-heuristic optimization algorithm proposed by Mirjalili et al. [34] in 2016. WOA algorithm mimics the hunting behavior of humpback whales with two phases; the exploitation phase which consists search for prey and the exploitation phase which regroups encircling prey and bubble-net attacking mechanism as illustrated in Fig. 5. For more details, the reader can refer to original paper [34].

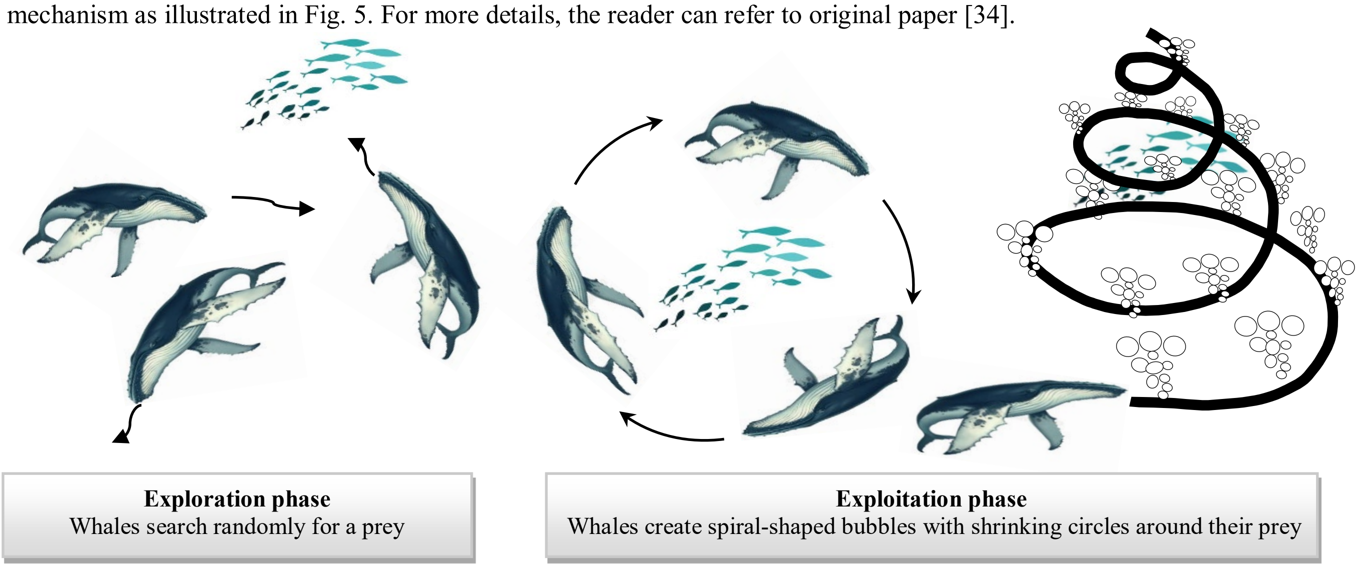

Fig. 5. The behavior of humpback whales in WOA algorithm.

IV PID/FOPID controller tuning using multi-objective optimization

In this section, the optimal tuning of the PID/FOPID controller's parameters using multi-objective optimization is presented. MOO is concerned with mathematical optimization problems involving more than one objective function to be optimized simultaneously. The result of MOO is expressed as a set of Pareto solutions, representing optimal trade-offs between different objectives. However, the main concern of the decision-maker is to find the best compromise solution from the Pareto front. A fuzzy decision-making approach is used in this paper to find the optimal Pareto point according to the decision-maker preferences [33].

This section presents, in the following subsections, objective functions, MOO approach steps and finally the adopted fuzzy decision-making method.

A) Objective functions

To approach the output system to its reference input, three objective functions are considered which are formulated based on:

1) **Settling time (ts)** is defined as the time for the response to reach, and stay within, **2%** of its final value.

$$f_1 = ts$$

1) **Maximum overshoot (Mp)** is straight way difference between the magnitude of the highest peak of time response and magnitude of its steady state.

$$f_2 = Mp$$

2) **Steady-state error (ess)** is the difference between actual output and desired output at the infinite range of time.

$$f_3 = ess$$

The goal of multi-objective algorithm is to minimize the function

$$F(x) = \{f_1(x), f_2(x), f_3(x)\}$$

with $x = [K_p, K_i, K_d]$ or $x = [K_p, K_i, K_d, \lambda, \mu]$ for PID or FOPID controller parameters, respectively.
For BLDC motor [29], the inequality constraints are

$$\begin{cases} \text{ts} \leq 2\text{s} \\ \text{Mp} \leq 10\% \\ \text{ess} \leq 0.01\% \end{cases}$$

In search space

$$PID: \begin{cases} K_{p\_min} \leq K_p \leq K_{p\_max} \\ K_{i\_min} \leq K_i \leq K_{i\_max} \\ K_{d\_min} \leq K_d \leq K_{d\_max} \end{cases}$$

$$FOPID: \begin{cases} K_{p\_min} \leq K_p \leq K_{p\_max} \\ K_{i\_min} \leq K_i \leq K_{i\_max} \\ K_{d\_min} \leq K_d \leq K_{d\_max} \\ \lambda_{min} \leq \lambda \leq \lambda_{max} \\ \mu_{min} \leq \mu \leq \mu_{max} \end{cases}$$

Where K_{p_min}, K_{i_min}, K_{d_min} and K_{p_max}, K_{i_max}, K_{d_max} are the lower and upper limits of PID controller parameters. While K_{p_min}, K_{i_min}, K_{d_min}, λ_{min}, μ_{min} and K_{p_max}, K_{i_max}, K_{d_max}, λ_{max}, μ_{max} are the lower and upper limits of FOPID controller parameters.

B) Multi-objective optimization steps

The following steps shown in Fig. 6. describe the MOO formulation:

Step 1: Initialize the population.
Step 2: Calculate the objective functions for each individual in the population.
Step 3: Update the Pareto archive as following:
- ✓ Find the non-dominated solutions.
- ✓ Store and update the set of non-dominated solutions in Pareto archive.
- ✓ Check the archive, if it is full, apply grid mechanism.

Step 4: Increment iteration number,
If the criterion ($k \leq k_{max}$) has been satisfied, then:

- ✓ Select the leader.
- ✓ Update the population position by specified algorithm (WOA).
- ✓ Go to **Step 2**.

Otherwise, return the final Pareto archive.
endif

For MOO, the Multi-Objective Whale Optimization Algorithm (MOWOA) is employed. This multi-objective algorithm was suggested recently by Kumawat et al. [35] based on original WOA [34].

C) Fuzzy Decision-Making

Once the Pareto front is obtained by MOO, it's time to extract the best compromise solution satisfying the desired goals [33]. To do this, a fuzzy decision-making procedure is implemented which the main steps, as shown in Fig. 7, are:

1) Prepare the inputs by normalizing all non-dominated solutions as follows [36]

$$u_i^j = \frac{f_i^{max} - f_i^j}{f_i^{max} - f_i^{min}} \; for \; i = 1,2,3 \; and \; j = 1,2, \ldots n$$

where, u_i^j indicates the normalized value of the non-dominated solution j of the objective function i, n is the number of nondominated solutions, f_i^{min} *and* f_i^{max} are the minimum and maximum value of the i^{th} objective function among all nondominated solutions of Pareto front, respectively.
2) The normalized functions are fuzzified using three triangular membership functions (MFs) for each input as shown in Fig. 8.
3) The fuzzy output weighting of the Pareto solutions, noted W, are determined using the fuzzy rules given in Table 1.
4) W is deduced using the triangular MF of the output. For each solution in the Pareto front, W is a number in the range [0,1].

After applying the fuzzy decision-making on the Pareto front, the best solution will be the one that has the maximum weighting value.

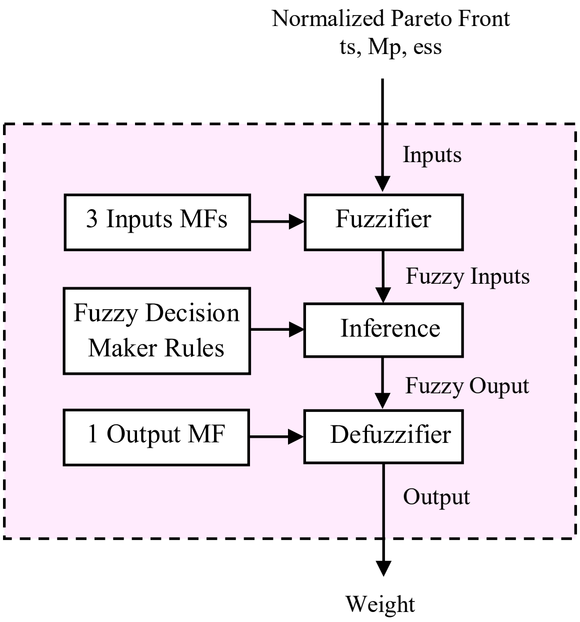

Fig. 7. Fuzzy decision-making steps.

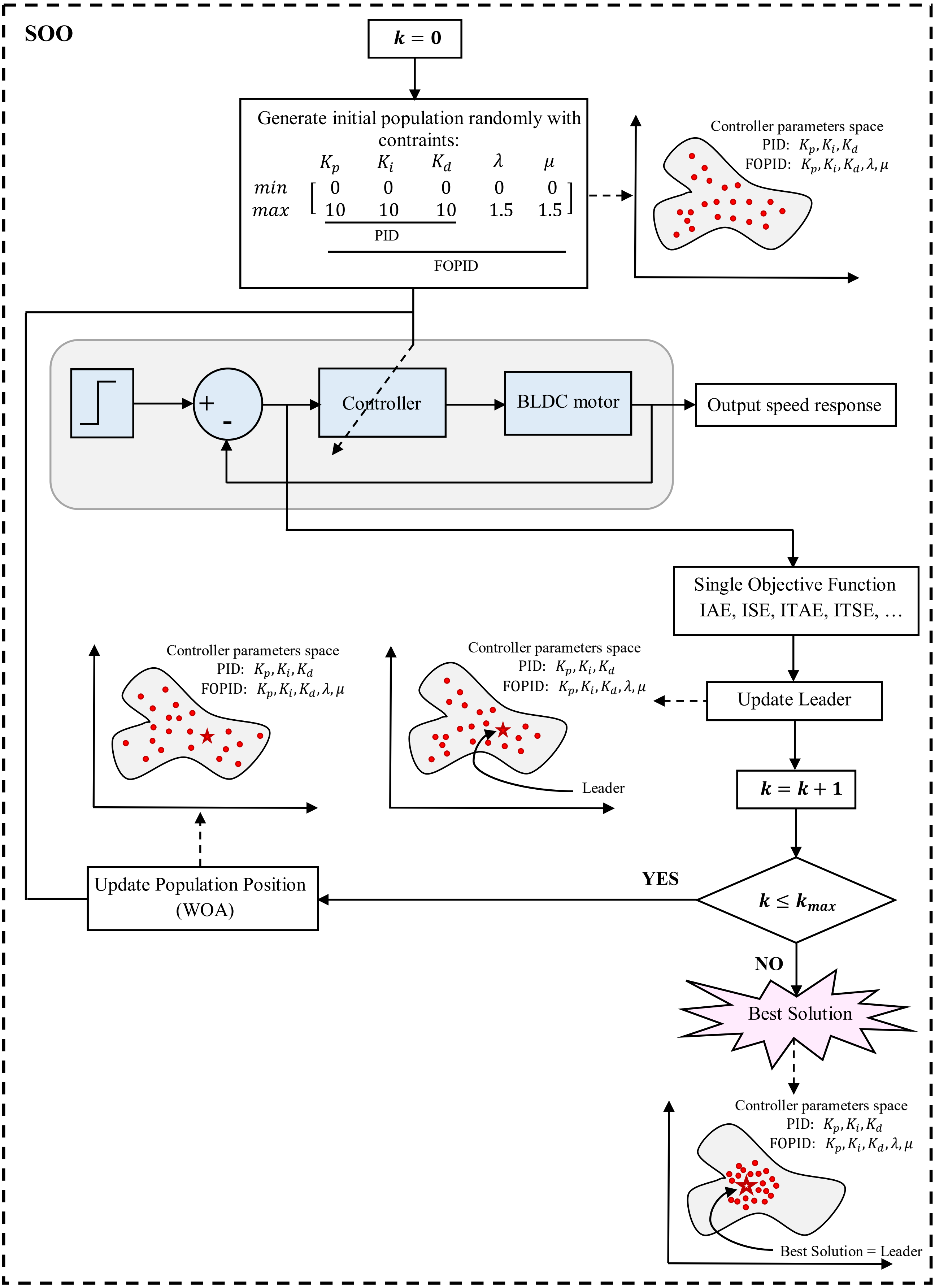

Fig. 4. PID/FOPID controllers tuning with single-objective optimization using WOA algorithm.

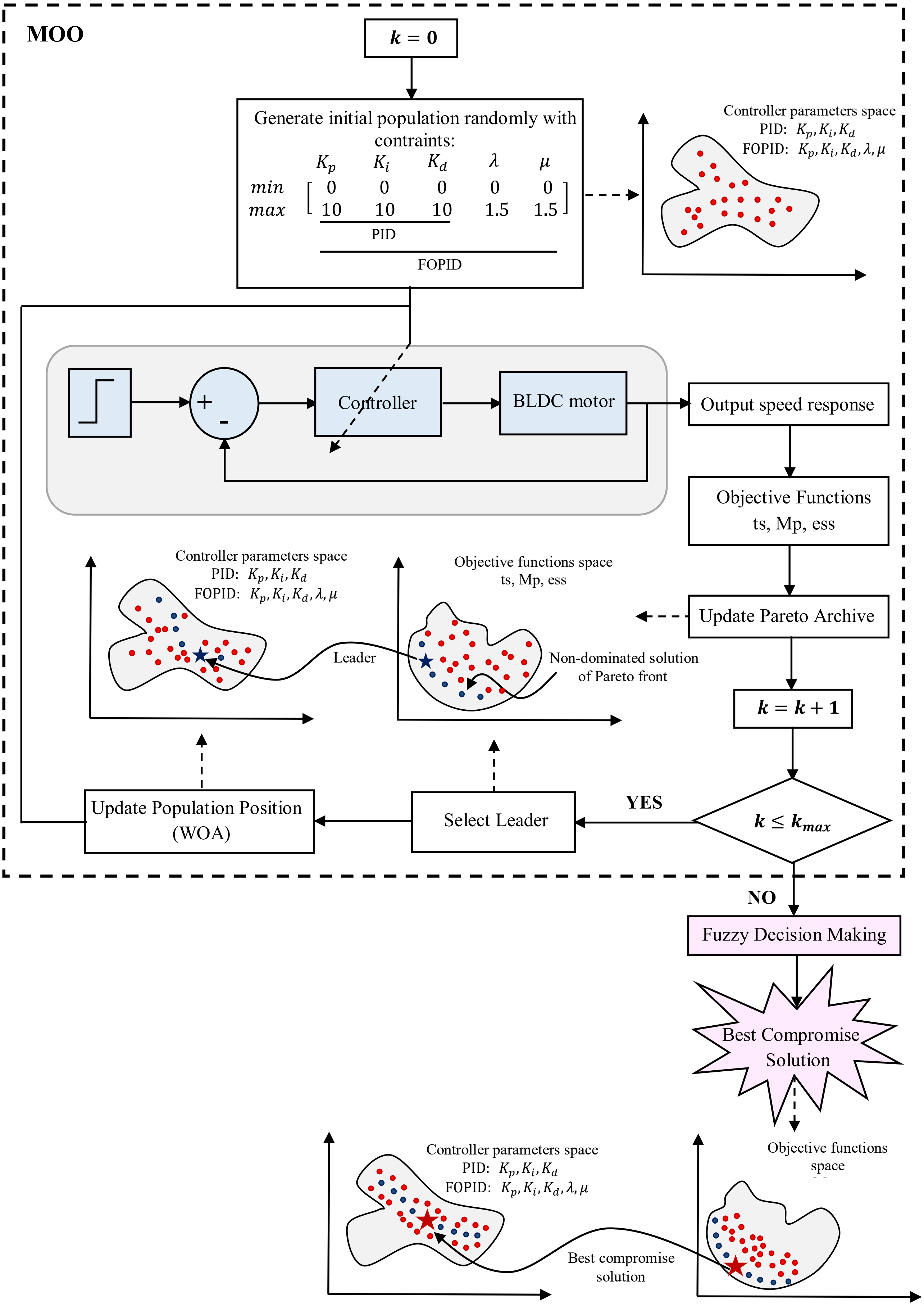

Fig. 6. PID/FOPID controllers tuning with multi-objective optimization using MOWOA algorithm.

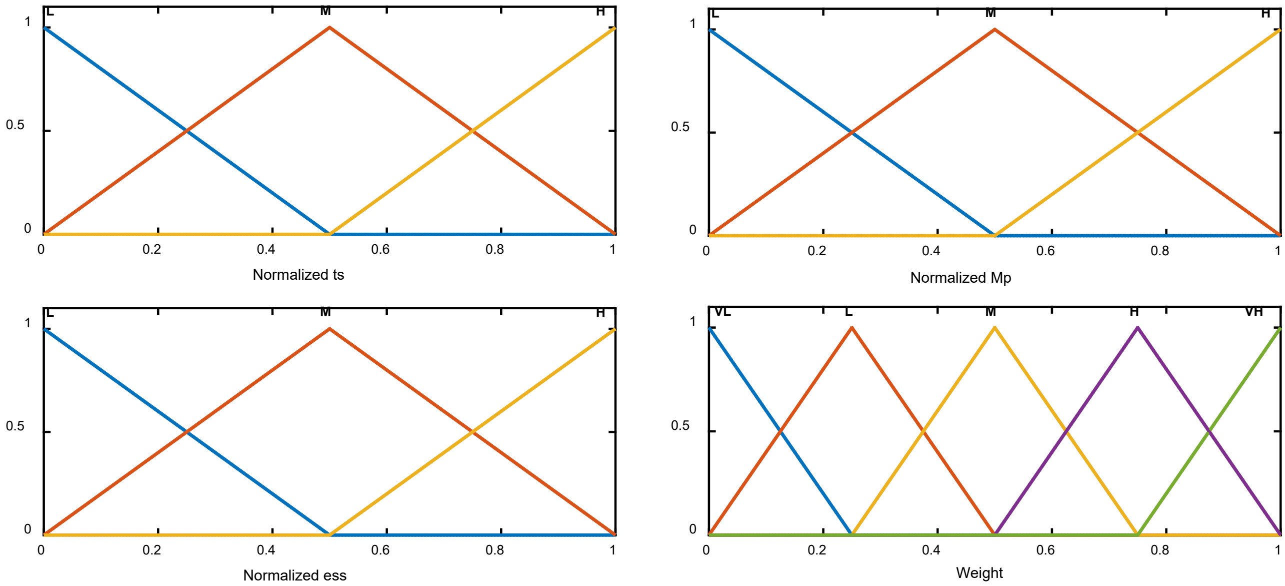

Fig. 8. Fuzzy membership degrees for normalized Inputs/Output.

Tab. 1. Fuzzy logic decision-making rules (VL =Very Low, L= Low, M= Medium, H= High, and VH= Very High).

ts	Mp	ess	W
H	H	H	VH
H	H	M	H
H	M	H	
M	H	H	
M	M	M	M
M	M	H	
M	H	M	
H	M	M	
L̄	L	X	L
L	X	L̄	
X	L̄	L	
L	L	L	VL

V Simulation and results

In order to compare the different PID/FOPID controllers tuned by single- and multi-objective optimization using WOA and MOWOA algorithms, step responses, frequency responses, tracking and load disturbance responses were all carried out and analyzed. The simulations of different responses were performed by means of the MATLAB/Simulink software package via a personal computer CORE i7 CPU with 8GB RAM. For FOPID, FOMCON toolbox [37] is integrated. In Oustaloup's approximation, $\omega_l = 10^{-3}$, $\omega_h = 10^{+3}$ and the order of approximation N is 5. The parameters values of the used algorithms are mentioned in Table 2.

Tab. 2. Parameters of WOA/MOWOA algorithms.

Parameter	Value
Poplation number	25
Iterations number	200
Min $[K_p\ K_i\ K_d\ \lambda\ \mu]$	[0 0 0 0 0]
Max $[K_p\ K_i\ K_d\ \lambda\ \mu]$	[10 10 1 1.5 1.5]
WOA: b	1
MOWOA: Multi-Objective optimization parameters	
Pareto archive size	100
grids number per dimension	10
inflation rate	0.1
leader selection pressure	4
Deletion selection pressure	2

The important results of this study are shown in the following subsections.

A) Speed comparison of BLDC motor with various controllers

For SOO, the results are obtained for 10 independent runs. At the end of the optimization process, the best convergence of ITAE objective function for PID/FOPID controller is obtained as shown in Fig. 9. As can be seen from the figure, the FOPID controller has the lowest ITAE value. Furthermore, Boxplot graphs of ITAE for PID/FOPID obtained so far over 10 independent runs are illustrated in Fig. 10. It is clear that ccompared with conventional PID controller, FOPID controller offers much more versatility in tuning because it has a large area of parameters that govern the controlled system which increases the reliability of the control loop. The obtained WOA-PID and WOA-FOPID controller's parameters are respectively: $K_p = 2.2183$, $K_i = 6.9518$, $K_d = 0.4119$ and $K_p = 5.5376$, $K_i = 9.9972$, $K_d = 0.4668$, $\lambda = 1.0097$, $\mu = 1.3516$.

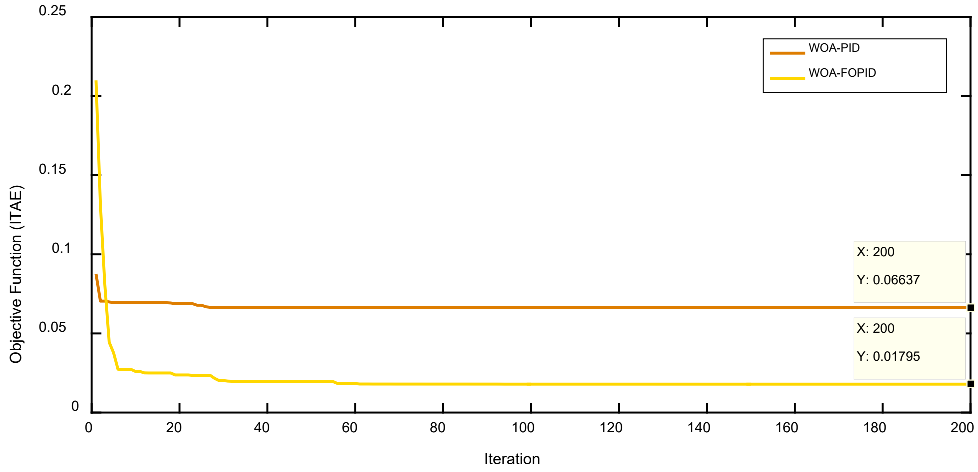

Fig. 9. Convergence of ITAE objective function for PID/FOPID controllers.

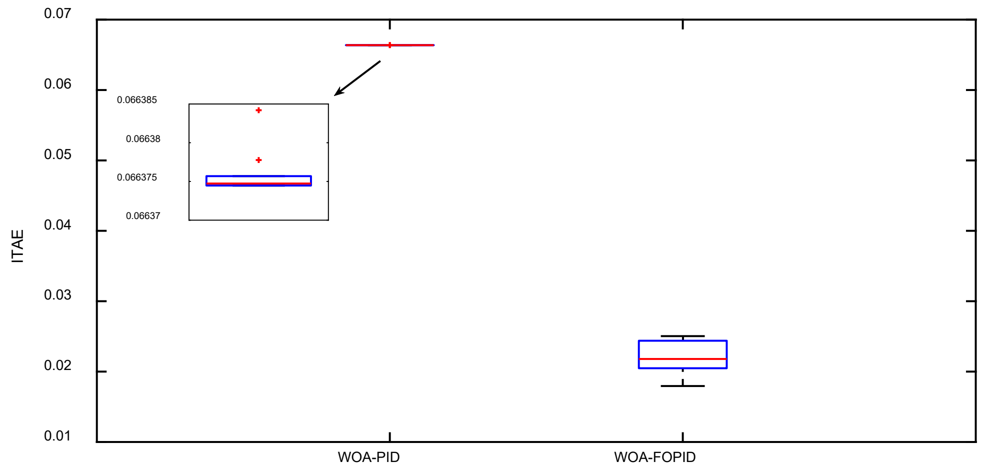

Fig. 10. Boxplots of ITAE objective function for PID/FOPID controllers over 10 independent runs.

For MOO, at the end of execution, MOWOA algorithm generates a set of solutions, i.e. optimized Pareto front. Fig. 11 illustrates the optimized Pareto fronts for PID and FOPID controllers. Besides, the figure shows for each controller the best compromise solution obtained applying fuzzy decision-making which corresponds to three objective functions. The best compromise solution for MOWOA-PID controller obtained with output weight $\mathrm{W} = 0.7688$ corresponds to: $\mathrm{ts} = 0.6624\ \mathrm{s}$, $\mathrm{Mp} = 1.3843$ and $\mathrm{ess} = 1.37\mathrm{e}-6$. That combination corresponds to MOWOA-PID parameters $K_p = 1.1189$, $K_i = 3.0017$, $K_d = 0.1125$. While the best compromise solution for MOWOA-FOPID controller obtained with output weight $\mathrm{W} = 0.8783$ corresponds to: $\mathrm{ts} = 0.2314\ \mathrm{s}$, $\mathrm{Mp} = 0$ and $\mathrm{ess} = 2.36\mathrm{e}-6$. That combination corresponds to MOWOA-FOPID parameters$K_p = 6.0993$, $K_i = 8.5166$, $K_d = 0.4572$, $\lambda = 1.0045$ and $\mu = 1.4230$.

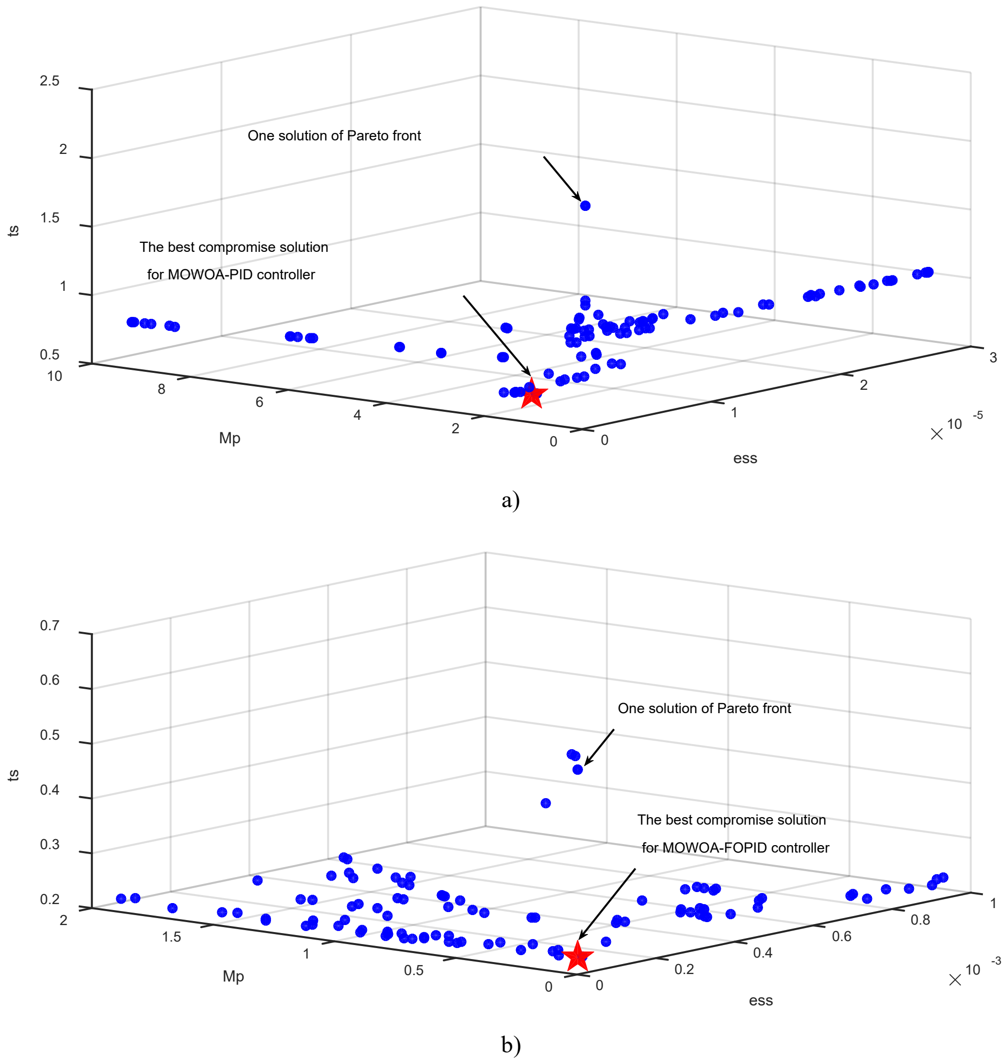

Fig. 11. Pareto front optimized with MOWOA: a) PID controller, b) FOPID controller.

Fig. 12 presents step responses of BLDC motor speed control systems with various controllers. Moreover, all these responses are grouped in Fig. 13. Table 3 gives PID/FOPID controllers parameters optimized by WOA and MOWOA. For a comparative analysis, Table 4 gives step responses' performances with best results highlighted in bold. It is clear from this table that the MOWOA-FOPID controller provides the response of a better quality with faster speed without any overshoots to step reference.

Tab. 3. PID/FOPID controller's parameters using WOA and MOWOA algorithms.

Controller	K_p	K_i	K_d	λ	μ
WOA-PID	2.2183	6.9518	0.4119	1	1
WOA-FOPID	5.5376	9.9972	0.4668	1.0097	1.3516
MOWOA-PID	1.1189	3.0017	0.1125	1	1
MOWOA-FOPID	6.0993	8.5166	0.4572	1.0045	1.4230

Tab. 4. Step responses's performances.

	tr (s)	ts (s) (2%)	Mp (%)	ess
WOA-PID	0.2209	1.4299	11.9288	9.92e-6
WOA-FOPID	0.1519	0.4144	5.3051	1.91e-4
MOWOA-PID	0.4311	0.6624	1.3843	1.37e-6
MOWOA-FOPID	**0.1518**	**0.2314**	**0**	2.36e-6

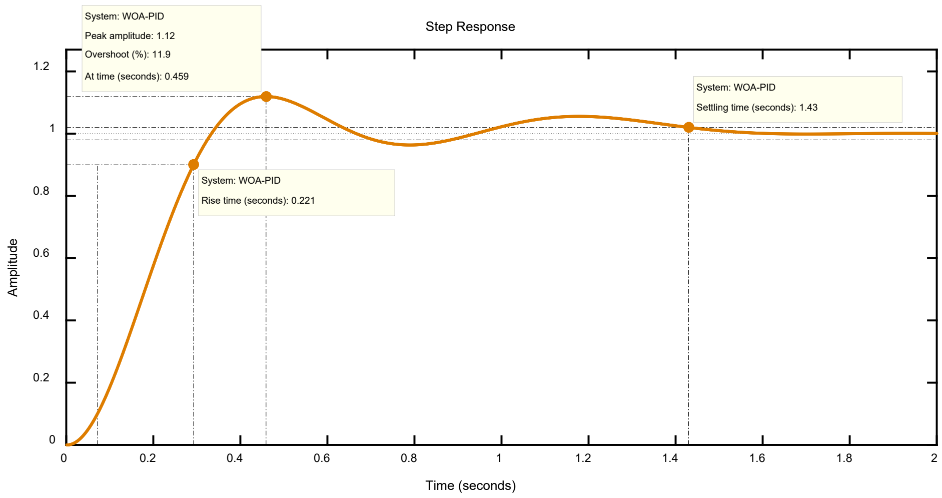
Step Response
System: WOA-PID
Peak amplitude: 1.12
Overshoot (%): 11.9
At time (seconds): 0.459
System: WOA-PID
Settling time (seconds): 1.43
System: WOA-PID
Rise time (seconds): 0.221
Amplitude
Time (seconds)

a)

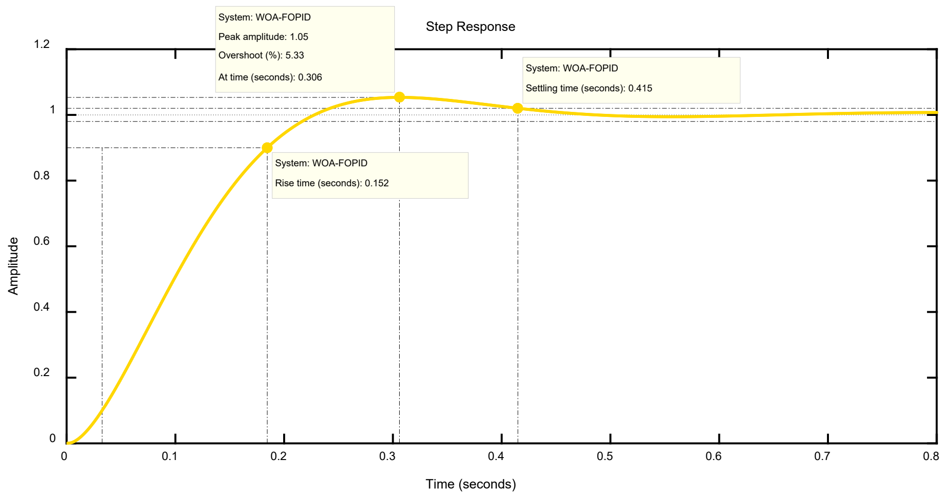
Step Response
System: WOA-FOPID
Peak amplitude: 1.05
Overshoot (%): 5.33
At time (seconds): 0.306
System: WOA-FOPID
Settling time (seconds): 0.415
System: WOA-FOPID
Rise time (seconds): 0.152
Amplitude
Time (seconds)

b)

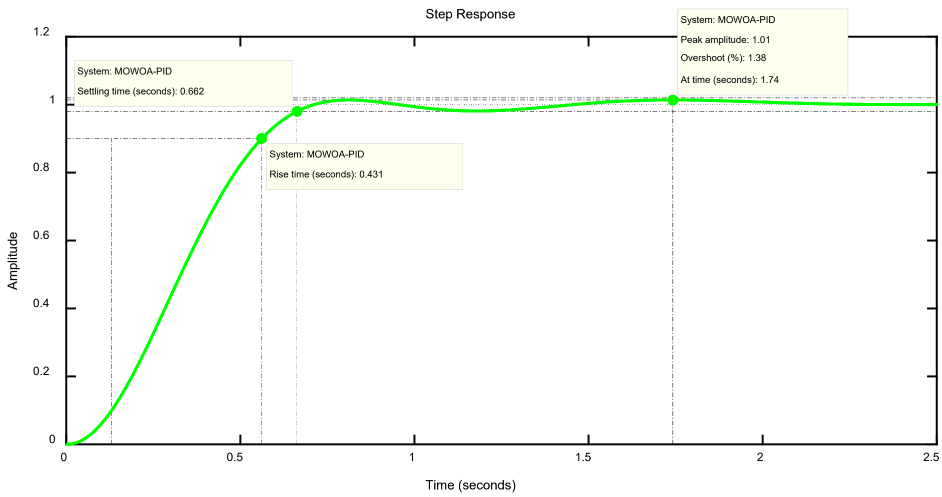
Step Response
System: MOWOA-PID
Peak amplitude: 1.01
Overshoot (%): 1.38
At time (seconds): 1.74
System: MOWOA-PID
Settling time (seconds): 0.662
System: MOWOA-PID
Rise time (seconds): 0.431
Amplitude
Time (seconds)

c)

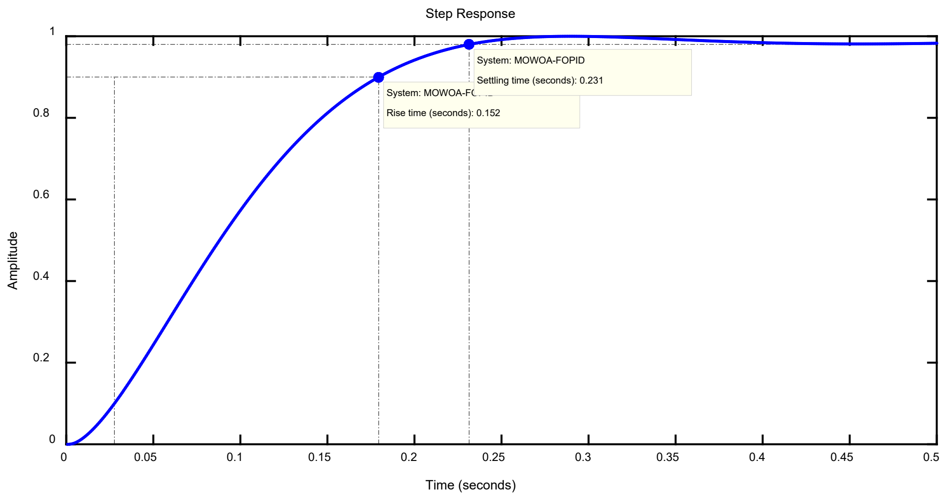

d)

Fig. 12. Step response of BLDC motor with different controllers:
a) WOA-PID, b) WOA-FOPID, c) MOWOA-PID, d) MOWOA-FOPID

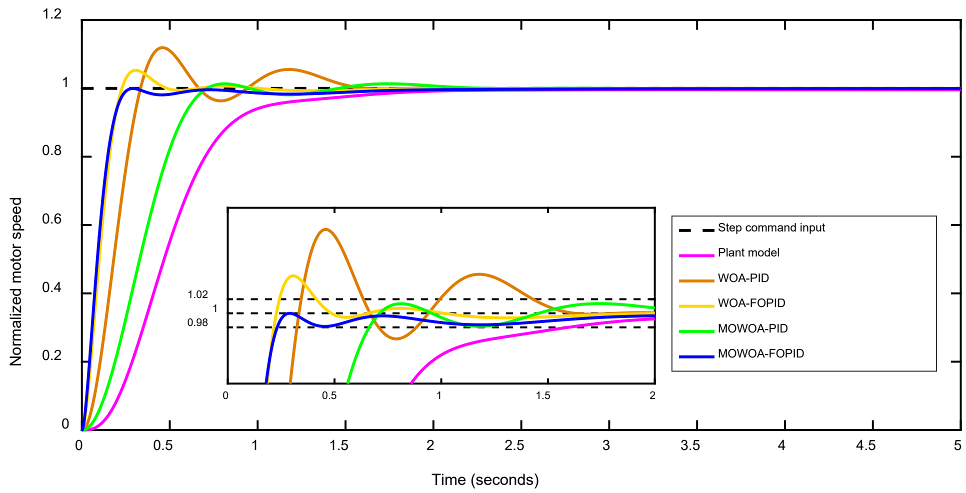

Fig. 13. Speed step responses of the BLDC motor control systems.

Fig. 14 shows the multi-step command-tracking responses of the BLDC motor speed control systems. Simulation results establish that MOWOA-FOPID provides better tracking capacity compared to other controllers.

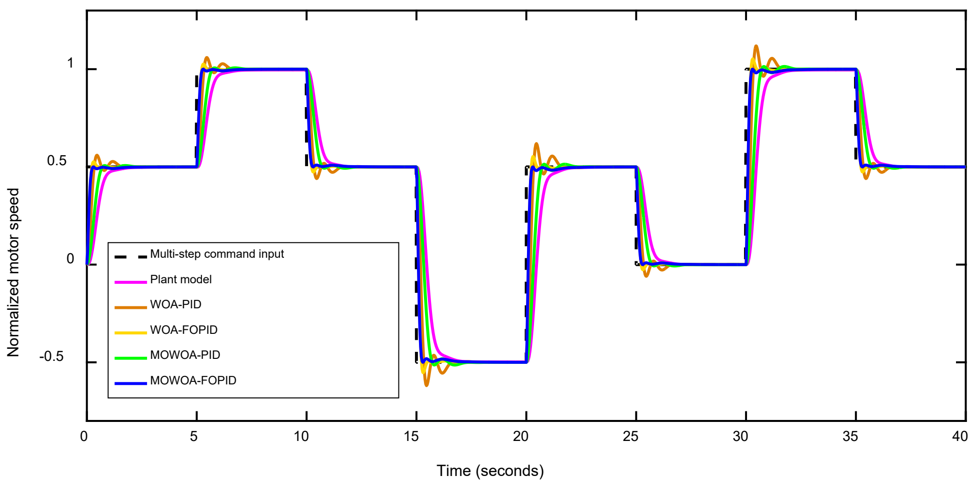

Fig. 14. Multi-step command-tracking responses of the BLDC motor speed control systems.

B) Frequency response analysis

To evaluate the stability performances of the BLDC motor speed control systems, the frequency responses were performed in Fig. 15 and 16 for open-loop and closed-loop control systems, respectively. For comparative analysis, the obtained performances of frequency responses are given in Table 5. As seen from the table, MOWOA-FOPID controller has the best performance with infinity gain margin, greater phase margin and bandwidth compared to other controllers. These results validate the effectiveness of the MOWOA-FOPID controller.

Tab. 5. Frequency response's performances.

Controller	GM (dB)	PM (deg)	Bandwidth (rad/s)
WOA-PID	∞	57.5926	10.3757
WOA-FOPID	∞	66.0288	14.0006
MOWOA-PID	137.3066	69.2599	5.69840
MOWOA-FOPID	∞	**73.0123**	**14.3270**

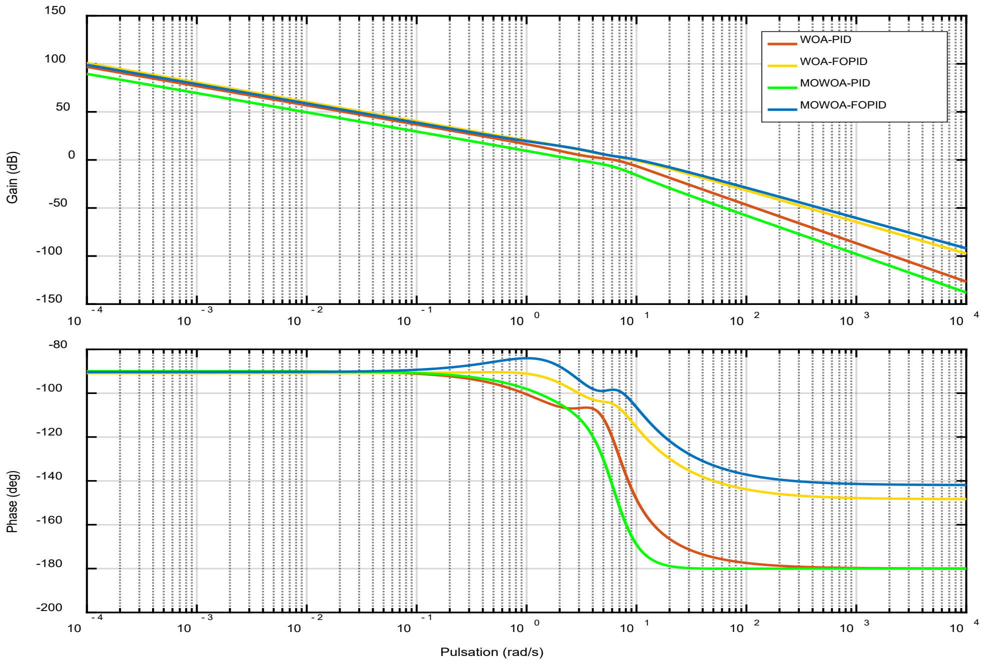

Fig. 15. Open-loop Bode plot of BLDC motor speed control system with different controllers.

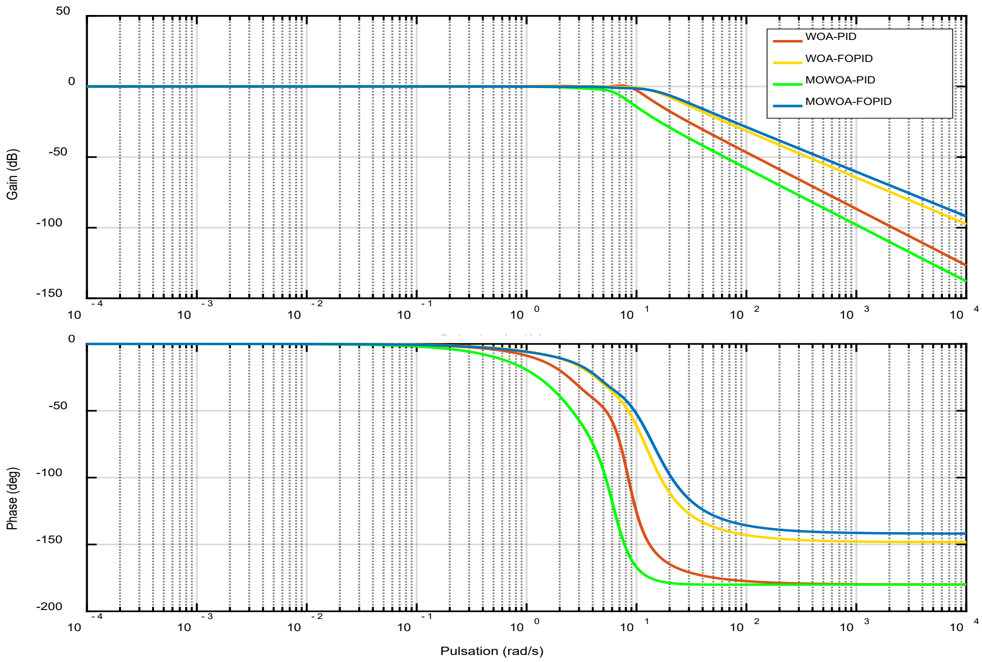

Fig. 16. Closed-loop Bode plot of BLDC motor speed control system with different controllers.

C) Load disturbance response

This subsection presents the rejection capability of the closed loop BLDC motor speed control system with the proposed controllers that are tested under the step load disturbance. Thanks to controllers, when a change in load occurs in the BLDC motor, the output speed response has to be settled down to zero as soon as possible. Fig. 17 shows the responses of the BLDC motor speed control for a step load disturbance and the responses' performances are given in Table 6. It is clear that the MOWOA-FOPID controller has the best load disturbance response in term of minimum overshoot with good settling time, compared to the other controllers. Hence, MOWOA-FOPID controller is more effective in suppressing the load disturbances. Moreover, the responses of speed for a multi-step load disturbance are presented in Fig. 18.

Tab. 6. Step load disturbance response's performances.

Controller	Settling time (s) (2%)	Overshoot (%)	ess
WOA-PID	1.7340	28.8700	**2.67e-6**
WOA-FOPID	**1.0080**	16.7830	1.91e-4
MOWOA-PID	1.7610	47.6276	8.95e-6
MOWOA-FOPID	1.1320	**16.0800**	1.08e-4

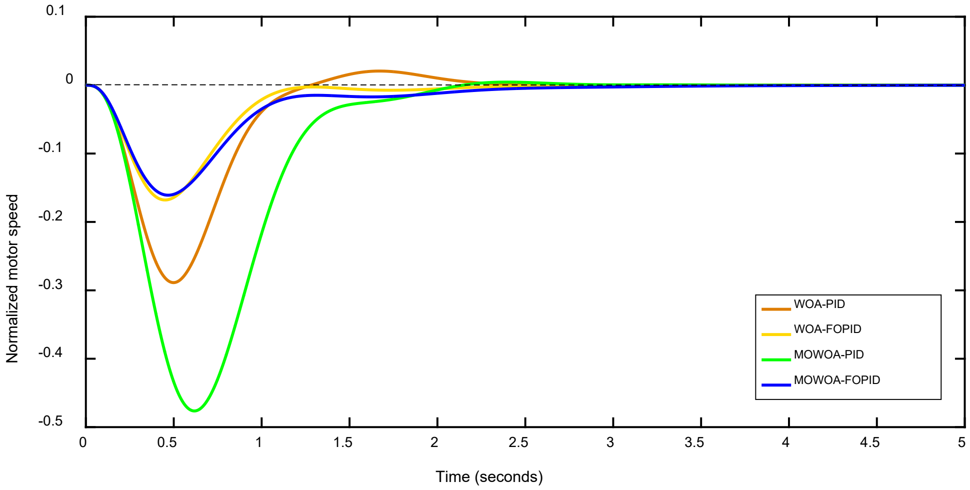

Fig. 17. Speed response of the BLDC motor with Unit-step load-disturbance.

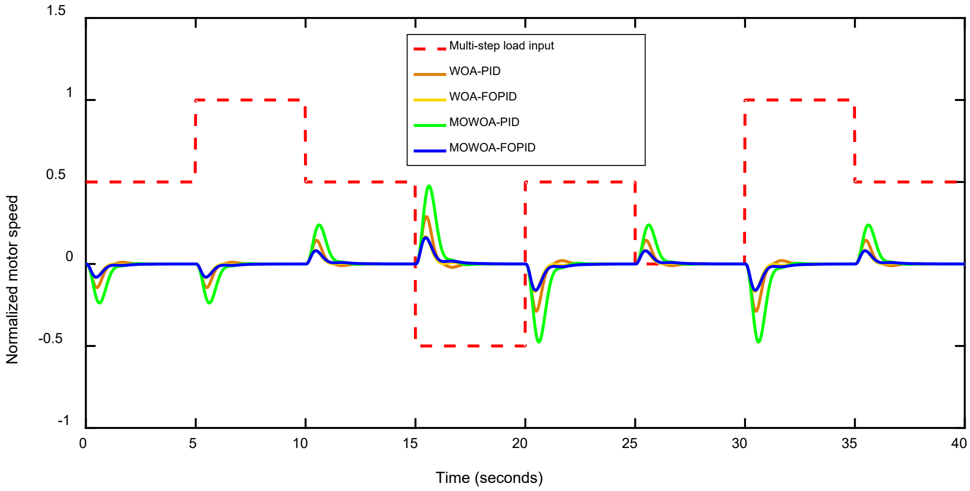

Fig. 18. Speed response of the BLDC motor with Multi-step load-disturbance.

VI Conclusion

In this paper, the optimal design of PID/FOPID controller parameters for speed control of BLDC motor is presented. The controller's parameters are tuned through single- and multi-objective optimization algorithms which are

WOA and MOWOA, respectively. For SOO, ITAE was taken as the main objective function to minimize. The best solution which corresponds to PID/FOPID controller's gains values has been obtained directly according to the minimum value of ITAE. While for MOO, three objective functions to minimize are employed which are: settling time, overshoot and error steady state. The best solution is determined by fuzzy logic-decision approach from the Pareto front archived by MOO. The simulation results reveal that the MOWOA-FOPID control system have good dynamic response capability; no overshoot, less settling and rise times in comparison with other controllers. As well, it is the more effective in good tracking capacity rejecting of the load disturbances. The performance of the MOWOA-FOPID controller has been also observed in the frequency domain responses with greater gain margin, phase margin and bandwidth.

In further works, we plan to optimize the FOPID controller for control systems by using hybridized algorithms [38] which offers superior performance compared to stand-alone algorithms. The mixed algorithms perform better because they choose the good algorithms attributes to improve on the vulnerabilities that exist in individual algorithms [19].

Declarations

Conflict of interest statement
The authors declare no conflict of interest in preparing this article.

Availability of data and materials
Not applicable.

Funding
This research received no specific grant from any funding agency in the public, commercial, or not-for-profit sectors.

References

[1] P. Yedamale, Brushless DC motor fundamentals, *Microchip Technology Incorporated*, 2003.
[2] K. Vanchinathan and N. Selvaganesan, Adaptive fractional order PID controller tuning for brushless DC motor using artificial bee colony algorithm, *Results. Control. Optim.*, 4: 100032, 2021.
[3] E. H. E. Bayoumi and H. M. Soliman, PID/PI tuning for minimal overshoot of permanent-magnet brushless DC motor drive using particle swarm optimization, *Electromotion Sci. J.*, 14(4): 198-208, 2007.
[4] A.M. Ahmed, A. Ali-Eldin, M.S. Elksasy and F.F. Areed, Brushless dc motor speed control using both PI controller and fuzzy PI controller, *Int. J. Comput. Appl.*, 109(10) : 29-35, 2015.
[5] W. Xie, J-S. Wang and H-B. Wang, PI controller of speed regulation of brushless DC motor based on particle swarm optimization algorithm with improved inertia weights, *Math. Probl. Eng.*, 2019: 2671792.
[6] H. Jigang, F. Hui, and W. Jie, A PI controller optimized with modified differential evolution algorithm for speed control of BLDC motor, *Automatika*, 60(2): 135-148, 2019.
[7] K. Premkumar and B. V. Manikandan, Bat algorithm optimized fuzzy PD based speed controller for brushless direct current motor, *Eng. Sci. Technol. an Int. J.*, 19(2): 818-840, 2016.
[8] M. Nasri, H. Nezamabadi-Pour and M. Maghfoori, A PSO-based optimum design of PID controller for a linear brushless DC motor. *World Acad. Sci., Eng Technol*, 26(40): 211-215, 2007.
[9] P. Sharma and G. Rajeev, Tuning of PID Controller for a linear brushless DC motor using swarm intelligence technique. *J. Eng. Res. Appl.*, 4(5) : 125-128, 2014.
[10] D. Potnuru and A.S.L.V. Tummala, Grey wolf optimization based improved closed-loop speed control for a BLDC motor drive, in *Proceedings of Smart Innovation, Systems and Technologies*, Vol. 104, pp. 145-152, 2019.
[11] M. Mahmud, S.M.A. Motakabber, A.H.M.Z. Alam and A.N. Nordin, Control BLDC motor speed using PID controller, *Int. J. Adv. Comput. Sci. Appl.*, 11(3): 477-481, 2020.
[12] M. Mahmud, S.M.A. Motakabber, A.H.M.Z. Alam, A.N. Nordin and A.K.M. Ahasan Habib, Modeling and performance analysis of an adaptive PID speed controller for the BLDC motor, *Int. J. Adv. Comput. Sci. Appl.*, 11(7): 272-276, 2020.
[13] C.S.R. Reddy and M.S. Kalavathi, Performance analysis of BLDC motor drive using new simulation model with fuzzy and ANFIS speed controllers, *Glob. J. Res. Eng. F*, 14 (4): 13-20, 2014.
[14] K. Premkumar and B.V. Manikandan, Adaptive neuro-fuzzy inference system based speed controller for brushless DC motor, *Neurocomputing*, 138: 260-270, 2014.
[15] H. Ahmed and A. Rajoriya, A hybrid of sliding mode control and fuzzy logic control using a fuzzy supervisory switched system for DC motor speed control, *Turk. J. Electr. Eng. Comput. Sci.,* 25(3): 1993–2004, 2017.
[16] R. Amirthalingam, B. Mahadevan and K. Vijayarajan, Adaptive MF tuned fuzzy logic speed controller for BLDC motor drive using ANN and PSO technique, *J. Eng.*, 17: 3947-3950, 2019.
[17] C.S. Vishnu and Riya Mary Francis, Speed control of BLDC motor using a tuned LQR controller, *Int. J. Sci. Eng. Res.*, 3(8): 2347-3878, 2015.
[18] H. Hu, T. Wang, S. Zhao, and C. Wang, Speed control of brushless direct current motor using a genetic algorithm-optimized fuzzy proportional integral differential controller, *Adv. Mech. Eng.*, 11(11): 1-13, 2019.
[19] S. Oladipo, Y. Sun, and Z. Wang, Optimization of PID controller with metaheuristic algorithms for DC motor drives: Review, *Int. Rev. Electr. Eng.*, 15(5): 352-381, 2020.
[20] I. Podlubny, Fractional-order systems and $PI^{\lambda}D^{\mu}$-controllers, *IEEE Trans. Automat. Contr.*, 44(1): 208-214, 1999.
[21] S. Das, Functional fractional calculus, *2nd ed. New York, NY, USA: Springer*, 2011.
[22] M.V. Aware, A.S. Junghare, S.W. Khubalkar, A. Dhabale, S. Das and R. Dive, Design of new practical phase shaping circuit using optimal pole-zero interlacing algorithm for fractional order PID controller, *Analog. Integr. Circ. Sig. Process.,* 91: 131-145, 2017.

[23] A.S. Chopade, S.W. Khubalkar, A.S. Junghare, M.V. Aware and S. Das, Design and implementation of digital fractional order PID controller using optimal pole-zero approximation method for magnetic levitation system, *IEEE/CAA J. Autom. Sin.*, 5(5): 977-989, 2016.
[24] D. Xue, C. Zhao, and Y. Q. Chen, Fractional order PID control of A DC-motor with elastic shaft: A case study, in *Proceedings of the 2006 American Control Conference*, Minnesota, USA, 14-16 June 2006, pp. 3182-3187.
[25] Y. Luo and Y. Chen, Stabilizing and robust fractional order PI controller synthesis for first order plus time delay systems, *Automatica*, 48(9): 2159-2167, 2012.
[26] R.A. Krohling and J.P. Rey, Design of optimal disturbance rejection PID controllers using genetic algorithms. *IEEE Trans Evol Comput*, 5(1): 78-82, 2001.
[27] N. Aguila-Camacho, M.A. Duarte-Mermoud, Fractional adaptive control for an automatic voltage regulator, *ISA Trans*, 52(6): 807-15, 2013.
[28] A. Selim, S. Kamel, A.S. Alghamdi and F. Jurado, Optimal placement of DGs in distribution system using an improved harris hawks optimizer based on single- and multi-objective approaches. *IEEE Access*, 8: 52815-52829, 2020.
[29] P. Khluabwannarat and D. Puangdownreong, Design of fractional-order PID Controller for fractional-order System via fower pollination agorithm, in *Proceedings of 2019 2nd Artificial Intelligence and Cloud Computing Conference*, Kobe, Japan, 21-23 December 2019, pp. 191-196.
[30] K. Balamurugan and R. Mahalakshmi, Anfis-fractional order pid with inspired oppositional optimization based speed controller for brushless dc motor, *Int. J. Wavelets Multiresolut. Inf. Process.*, 18(01): 1941004, 1-18, 2020.
[31] S. Kamel, A. Selim, F. Jurado, J. Yu, K. Xie and C. Yu, Multi-objective whale optimization algorithm for optimal integration of multiple DGs into distribution systems, in *Proceedings of the 2019 IEEE Innovative Smart Grid Technologies-Asia (ISGT Asia)*, Chengdu, China, 21-24 May 2019, pp. 1312-1317.
[32] P. Khluabwannarat, A. Nawikavatan and D. Puangdownreong, Fractional-order model parameter identification of BLDC motor by flower pollination algorithm, *WSEAS Trans. Syst. Control.*, 13: 573-579, 2018.
[33] W. Ahmed, A. Selim, S. Kamel, J. Yu, and F. Jurado, Probabilistic load flow solution considering optimal allocation of SVC in radial distribution system, *Int. J. Interact. Multimed. Artif. Intell.*, 5(3): 152-161, 2018.
[34] S. Mirjalili and A. Lewis, The whale opitmization algorithm, *Adv. Eng. Softw.*, 95: 51-67, 2016.
[35] I.R. Kumawat, S.J. Nanda and R.K. Maddila, Multi-objective whale optimization, in *Proceedings of the TENCON 2017-2017 IEEE Region 10 Conference*, Penang, Malaysia, 5-8 November 2017, pp. 2747-2752.
[36] M. Sakawa, H. Yano, and T. Yumine, An interactive fuzzy satisficing method for multiobjective linear-programming problems and its application, *IEEE Trans. Syst. Man. Cybern.*, 17(4): 654-661, 1987.
[37] A. Tepljakov, E. Petlenkov, and J. Belikov, FOMCON: Fractional-Order Modeling and Control Toolbox for MATLAB, in *Proceedings of the 18th International Conference on Mixed Design of Integrated Circuits and Systems*, Gliwice, Poland, 16-18 June 2011, pp. 684-689.
[38] A.Boubidi, S.Kechida and S.Hassainia, A New Version Of Hybrid Grey Wolf Optimizer With Sine Cosine Algorithm (Ngwosca), Studies in Science of Science, 42(12):78-90, 2024.